# Supplementary Material

| BRANCH 7 | *LOW IC MOTIF* | *HIGH IC MOTIF* |
|---|---|---|
| *LOW IC MOTIF (to)* | -3.75 | -3.70 |
| *HIGH IC MOTIF (to)* | -3.74 | -3.73 |

| BRANCH 11 | *LOW IC MOTIF* | *HIGH IC MOTIF* |
|---|---|---|
| *LOW IC MOTIF (to)* | -3.77 | -3.74 |
| *HIGH IC MOTIF (to)* | -3.77 | -3.73 |

| BRANCH 19 | *LOW IC MOTIF* | *HIGH IC MOTIF* |
|---|---|---|
| *LOW IC MOTIF (to)* | -2.96 | -3.01 |
| *HIGH IC MOTIF (to)* | -2.88 | -2.96 |

| BRANCH 20 | *LOW IC MOTIF* | *HIGH IC MOTIF* |
|---|---|---|
| *LOW IC MOTIF (to)* | -3.80 | -3.78 |
| *HIGH IC MOTIF (to)* | -3.80 | -3.81 |

| BRANCH 33 | *LOW IC MOTIF* | *HIGH IC MOTIF* |
|---|---|---|
| *LOW IC MOTIF (to)* | -3.74 | -3.72 |
| *HIGH IC MOTIF (to)* | -3.74 | -3.76 |

| BRANCH 39 | *LOW IC MOTIF* | *HIGH IC MOTIF* |
|---|---|---|
| *LOW IC MOTIF (to)* | -3.65 | -3.67 |
| *HIGH IC MOTIF (to)* | -3.61 | -3.65 |

**Figure S1. Information content (IC) based distribution of rewiring scores per branch.** In each branch, we pooled rewiring scores based on whether the rewiring is between (1) a low IC motif-to-low IC motif, (2) a low IC motif-to-high IC motif, (3) a high IC motif-to-low IC motif, or (4) a high IC motif-to-high IC motif. These tables summarize the medians of each binned category per branch.

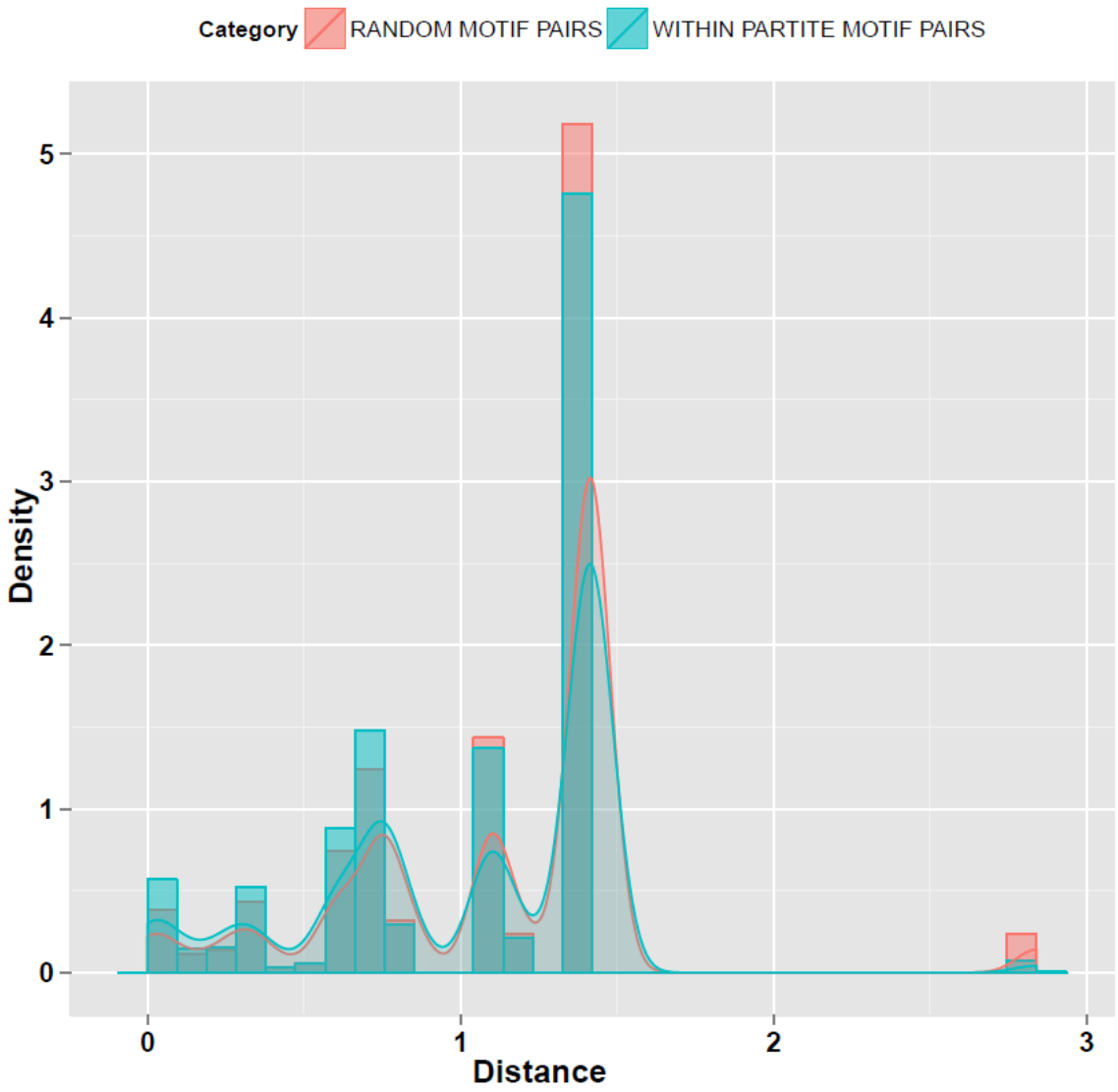


**Figure S2. Effect of motif similarity on detection of "multiplicity" of rewiring at regulons.** Overlapping histograms and density profiles of distance between consensus sequences of motifs (a proxy for pairwise motif similarity) of 1) TFs rewiring at the same regulon and the same branch (in blue), and 2) random TF pairs representing the background distribution of motif similarity across TFs (in pink).

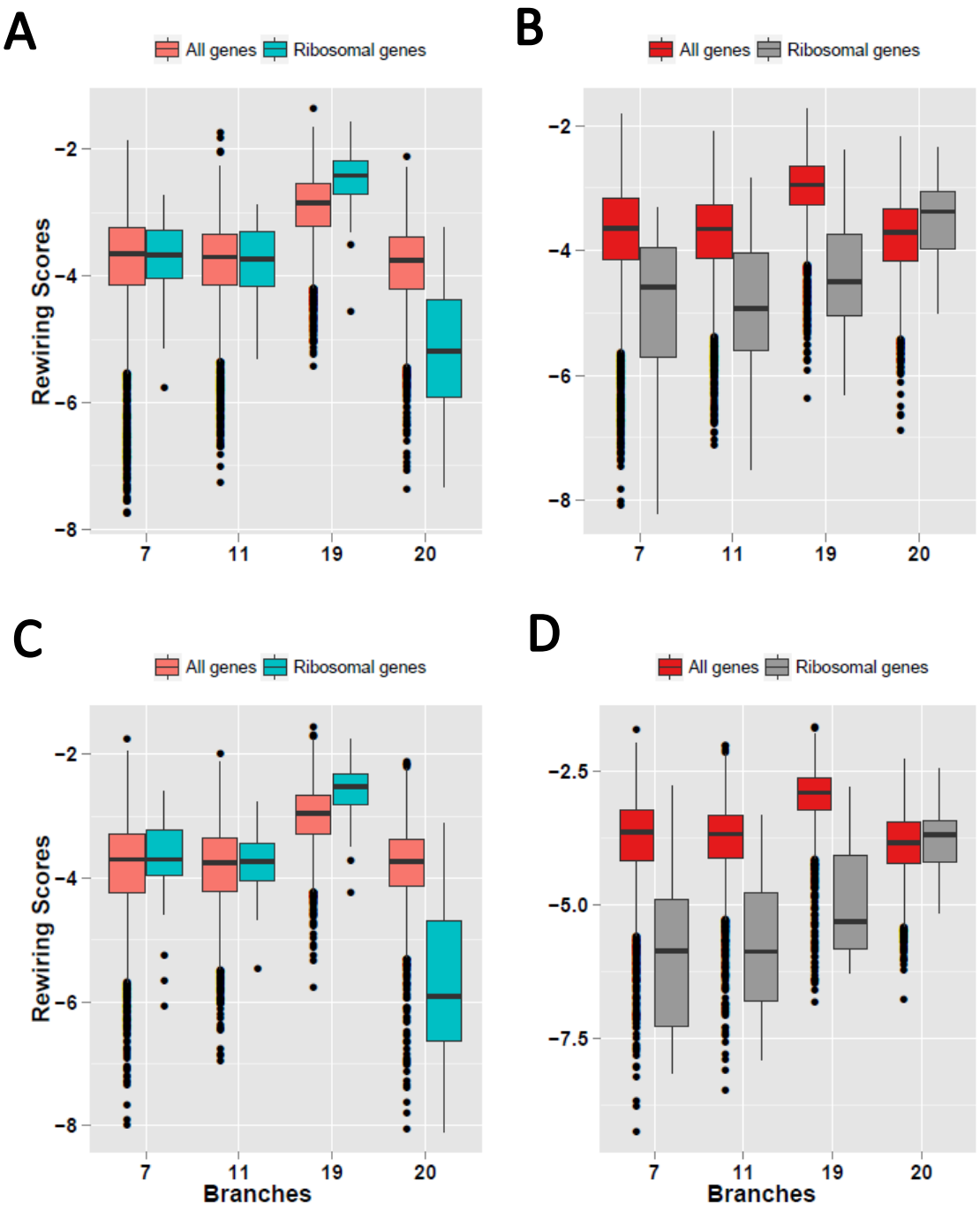


**Figure S3: Rewiring scores of the ribosomal regulon for *RAP1-CBF1* and *IFH1-TBF1* switches across branches.** The rewiring scores are shown on the Y axis, and the selected branches are shown on X axis. **(A)** *RAP1 in lineage & CBF1 in ancestral species*: This plot compares the rewiring score distribution of the background (all genes; in pink) and that of ribosomal genes (in blue) for the potential that *RAP1* regulates its member genes in species diverging from a given branch *b*, and *CBF1* regulates the ancestral species. **(B)** *CBF1 in lineage & RAP1 in ancestral species*: This plot compares the rewiring score distribution of the background (in red) and that of ribosomal genes (in grey) for the potential that *CBF1* regulates its member genes in species diverging from a given branch *b*, and *RAP1* regulates the ancestral species. **(C)** & **(D)** are analogous to (A) & (B) respectively for the *IFH1-TBF1* switch in RP genes.

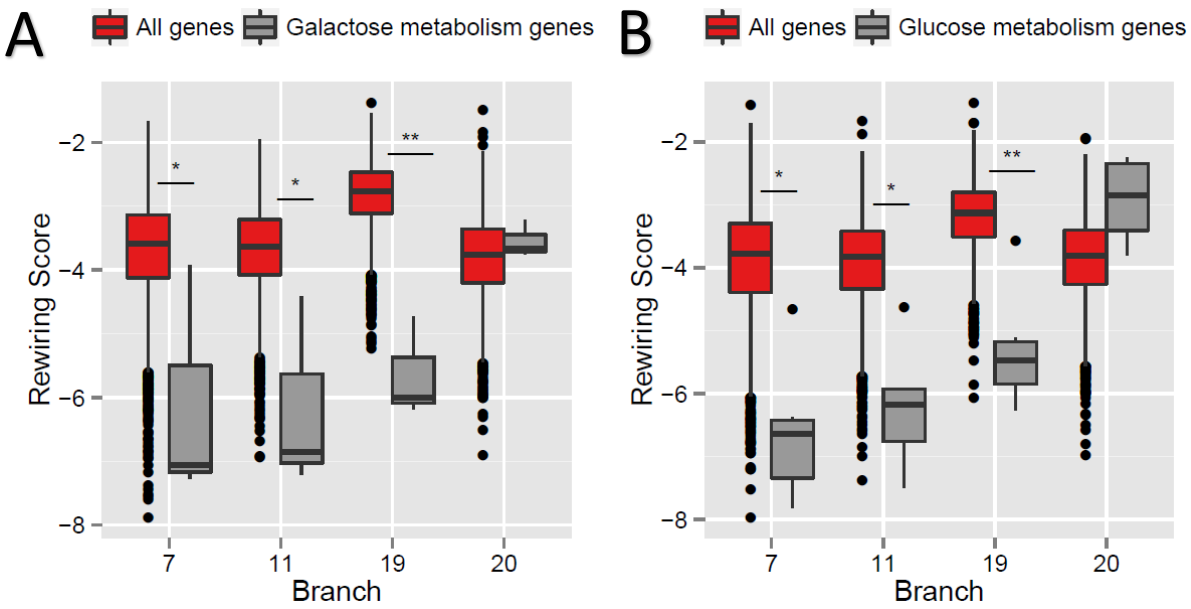


**Figure S4. Rewiring score distribution for complementary configurations (see Results for explanation) of known rewiring events across all branches.** The rewiring scores are shown on the Y axis, and the selected branches are shown on X axis. **(A)** *CPH1 in lineage & GAL4 in ancestral species*: This plot compares the rewiring score distribution of the background (all genes; in red) and that of galactose metabolism genes (in grey for the potential that *CPH1* regulates its member genes in species diverging from a given branch *b*, and *GAL4* regulates the ancestral species. **(B)** *GAL4 in lineage & GCR1 in ancestral species*: This plot compares the rewiring score distribution of the background (in red) and that of glucose metabolism genes (in grey) for the potential that *GAL4* regulates its member genes in species diverging from a given branch *b*, and *GCR1* regulates the ancestral species.

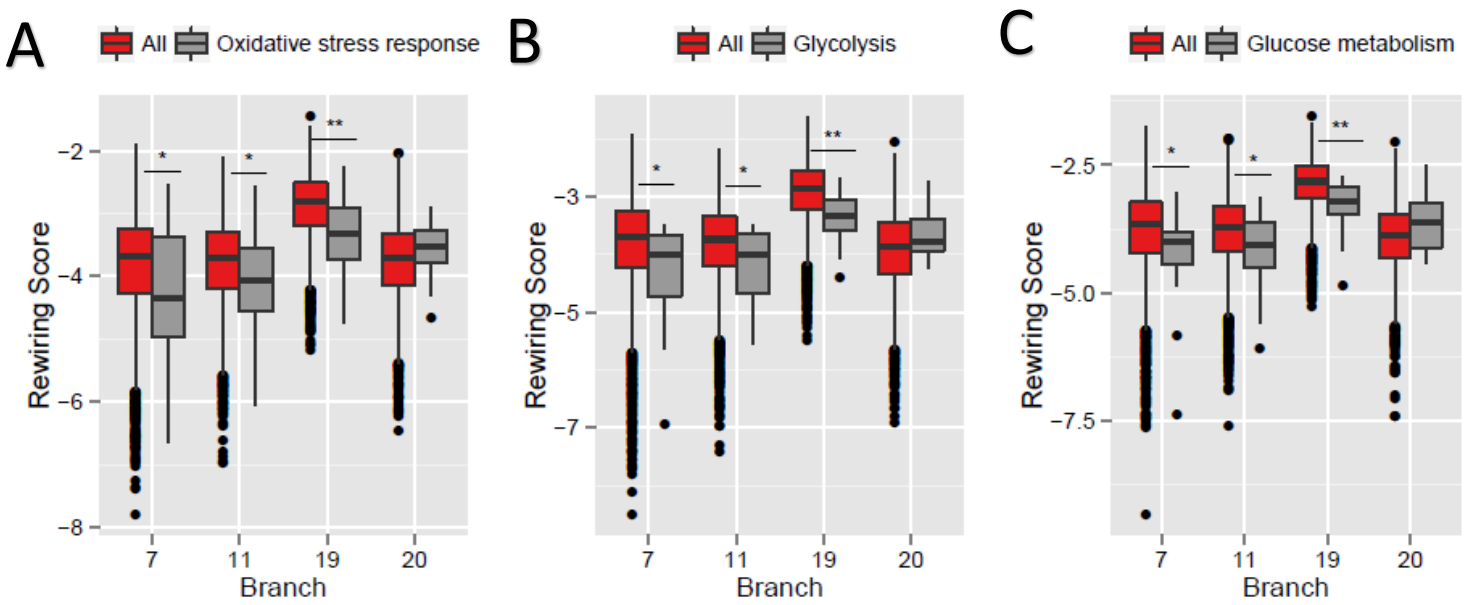


**Figure S5. Rewiring score distribution for complementary configurations (see Results for explanation) of predicted rewiring events across all branches.** See Legend S4 for details **(A)** Oxidative stress response genes regulation by *FKH2 in lineage & MSN2 in ancestral species* **(B)** Glycolysis genes regulation by *UME6 in lineage & RTG1 in ancestral species* **(C)** Glycolysis genes regulation by *GCN4 in lineage & RTG1 in ancestral species*

A

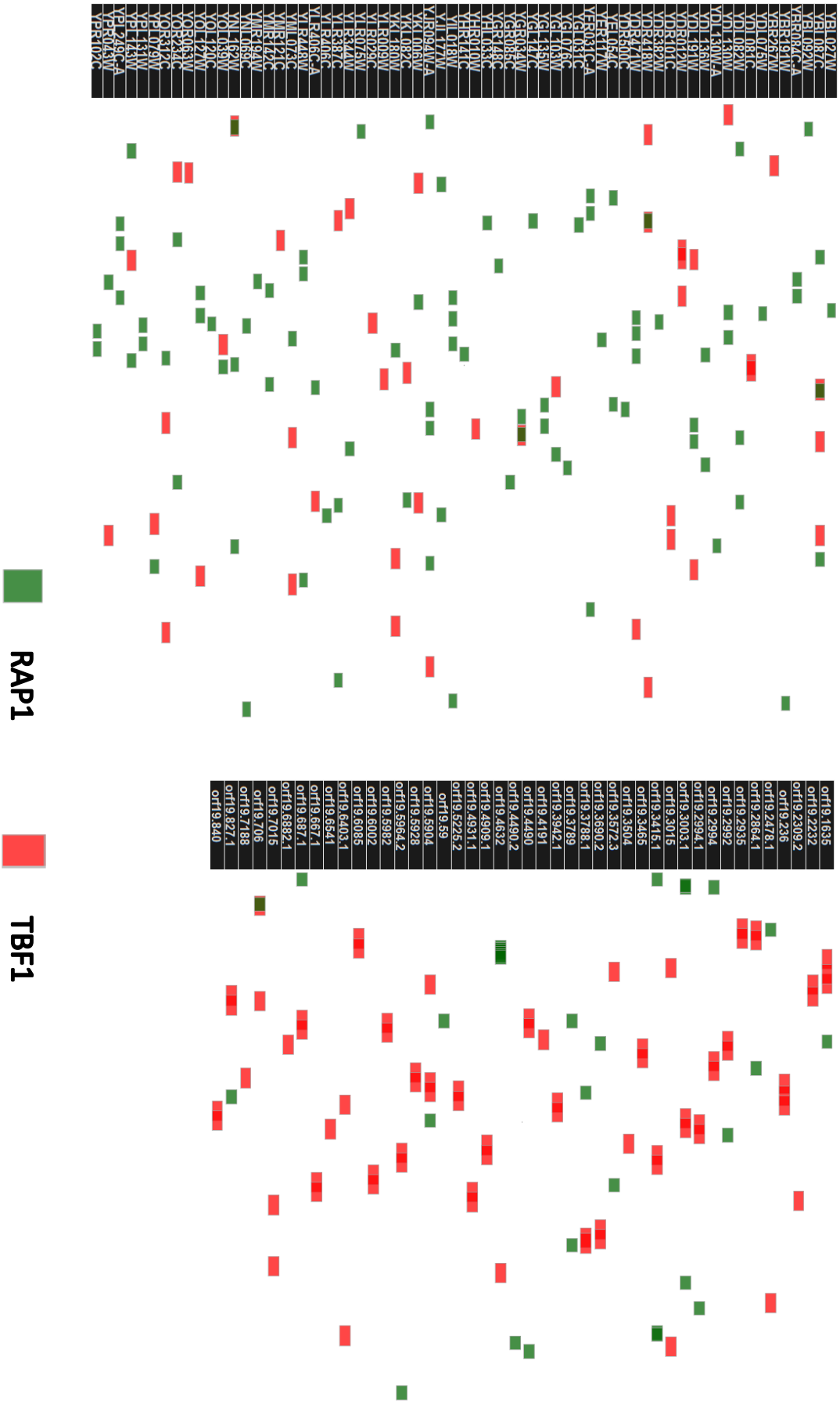

B


YBR018C
YBR019C
YBR020W
YDR009W
YHR210C
orf19.3672
orf19.3675
GAL4
CPH1

C

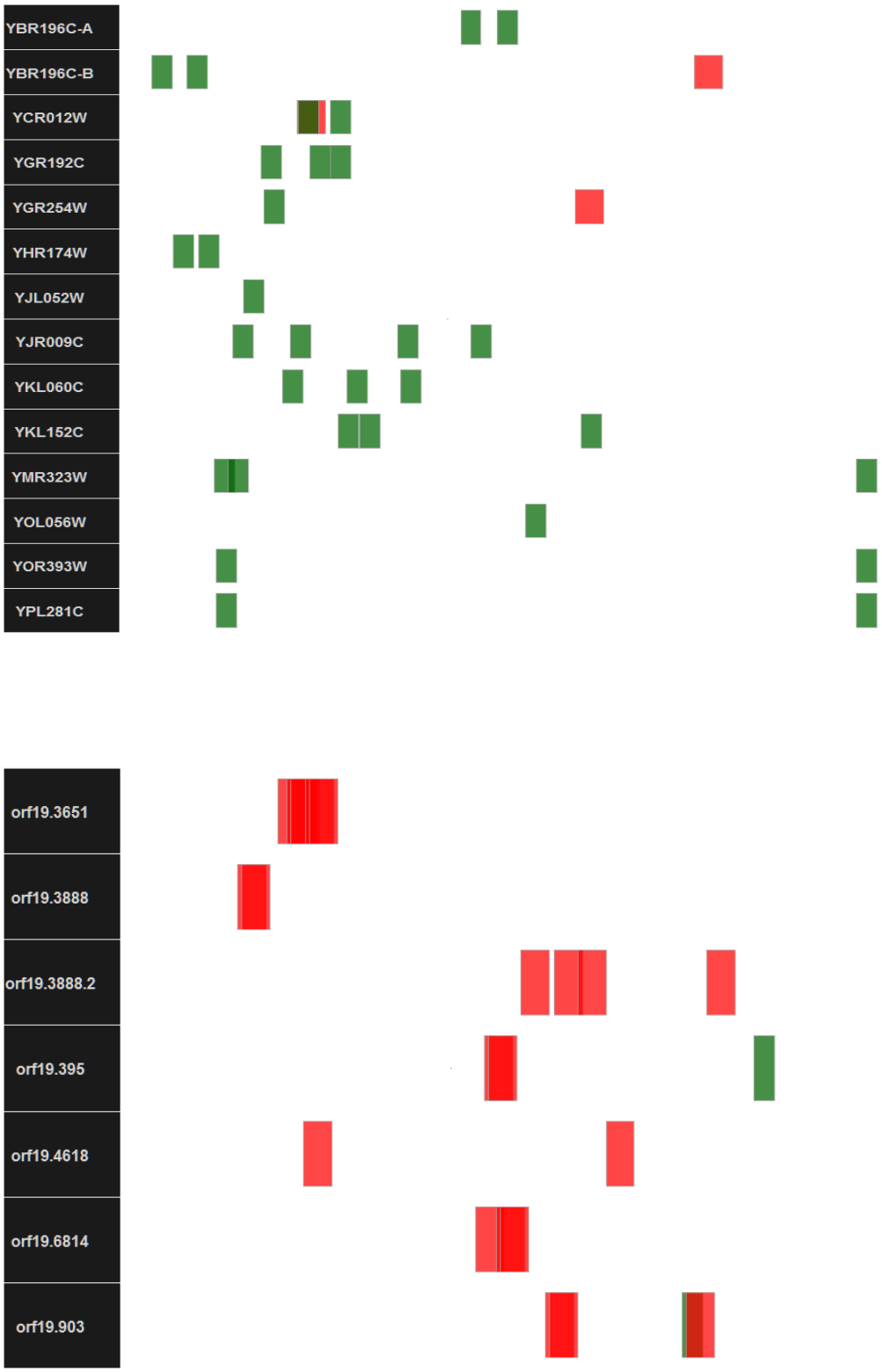
YBR196C-A
YBR196C-B
YCR012W
YGR192C
YGR254W
YHR174W
YJL052W
YJR009C
YKL060C
YKL152C
YMR323W
YOL056W
YOR393W
YPL281C
orf19.3651
orf19.3888
orf19.3888.2
orf19.395
orf19.4618
orf19.6814
orf19.903
GCR1
GAL4

D

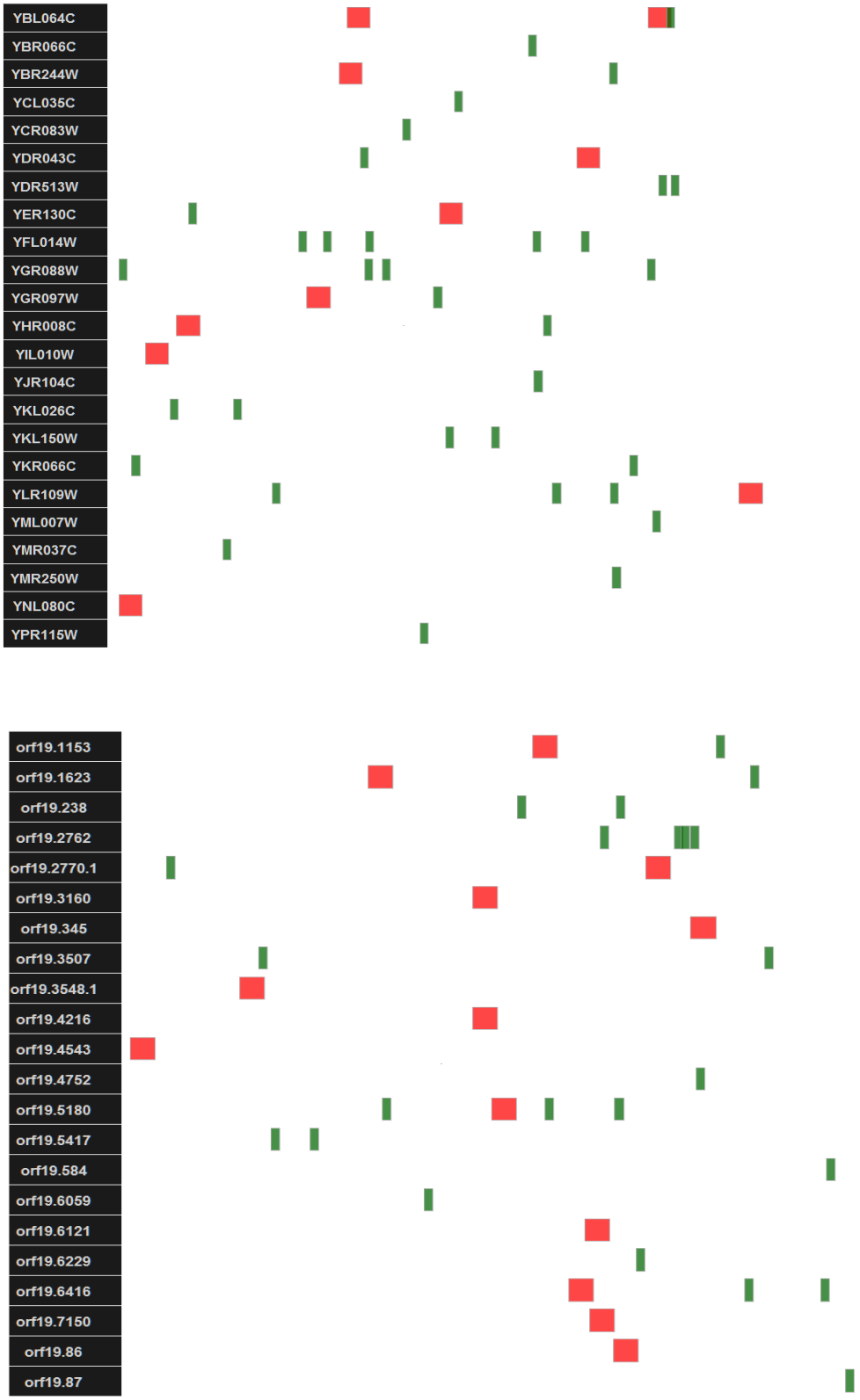
YBL064C
YBR066C
YBR244W
YCL035C
YCR083W
YDR043C
YDR513W
YER130C
YFL014W
YGR088W
YGR097W
YHR008C
YIL010W
YJR104C
YKL026C
YKL150W
YKR066C
YLR109W
YML007W
YMR037C
YMR250W
YNL080C
YPR115W
orf19.1153
orf19.1623
orf19.238
orf19.2762
orf19.2770.1
orf19.3160
orf19.345
orf19.3507
orf19.3548.1
orf19.4216
orf19.4543
orf19.4752
orf19.5180
orf19.5417
orf19.584
orf19.6059
orf19.6121
orf19.6229
orf19.6416
orf19.7150
orf19.86
orf19.87
MSN2
FKH2

E

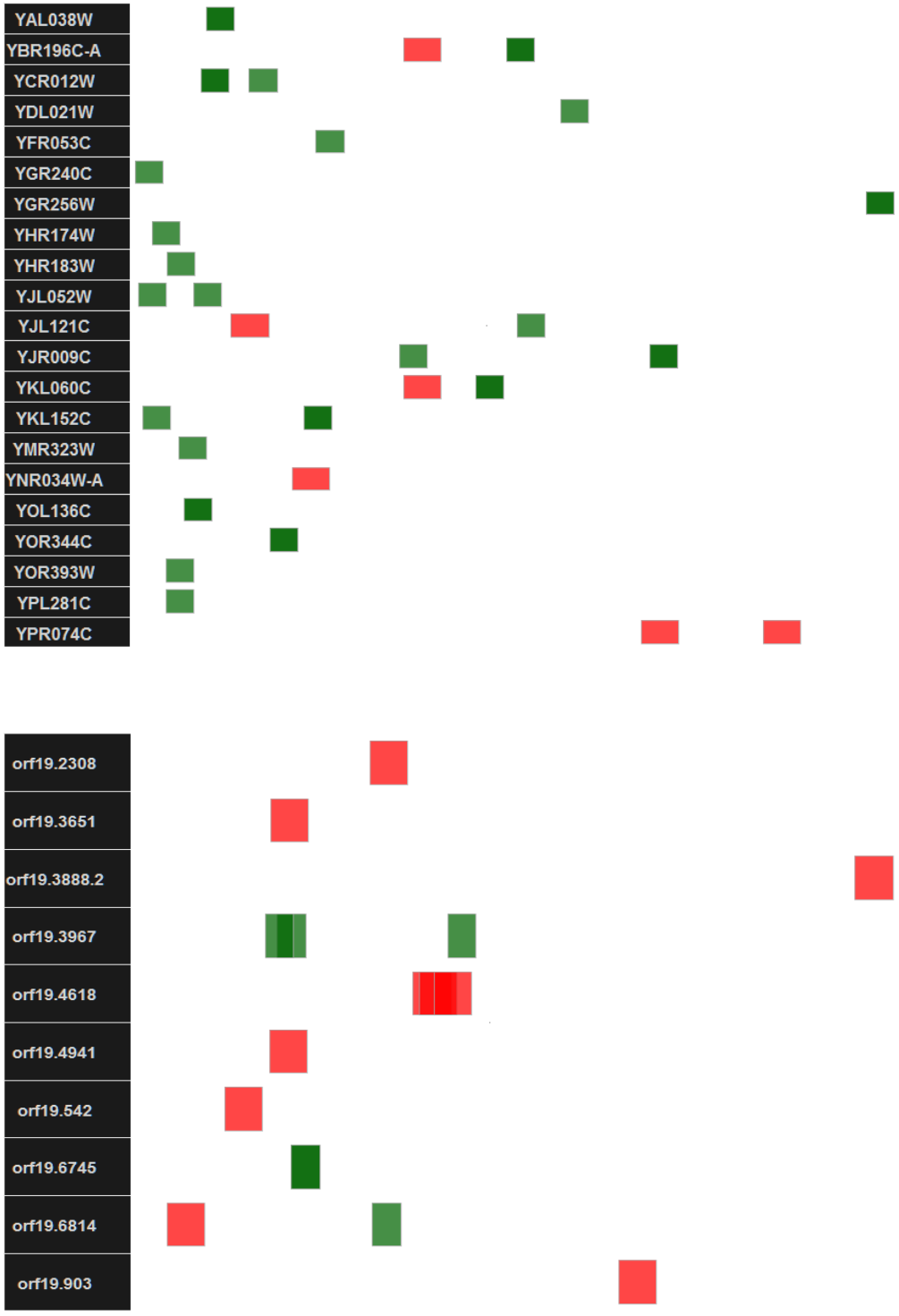
YAL038W
YBR196C-A
YCR012W
YDL021W
YFR053C
YGR240C
YGR256W
YHR174W
YHR183W
YJL052W
YJL121C
YJR009C
YKL060C
YKL152C
YMR323W
YNR034W-A
YOL136C
YOR344C
YOR393W
YPL281C
YPR074C
orf19.2308
orf19.3651
orf19.3888.2
orf19.3967
orf19.4618
orf19.4941
orf19.542
orf19.6745
orf19.6814
orf19.903
RTG1
GCN4

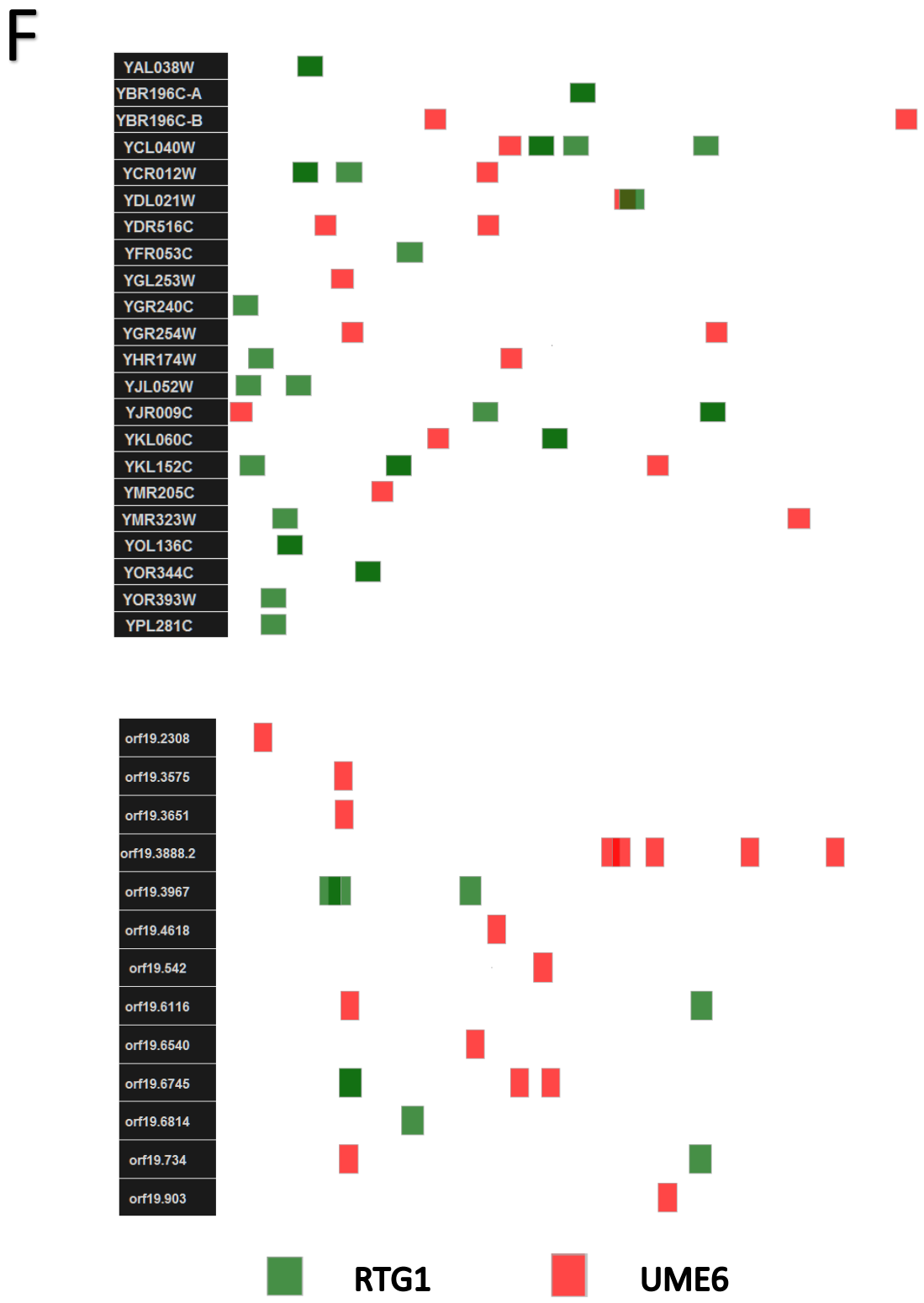


**Figure S6. TFBS profiles for regulons in *Scer* and *Calb* for each rewiring event discussed in the main text.** Each figure from (A) to (F) has two panels comprising of genes in regulons from (1) Scer, and (2) Calb. Each line represents a gene promoter labelled with Gene ID, with TFBS annotated across its sequence. (A) Ribosomal proteins regulon with TFBS profiles of RAP1 and TBF1, (B) Galactose metabolism regulon with TFBS profiles of GAL4 and CPH1, (C) Glucose metabolism regulon with TFBS profiles of GCR1 and GAL4, (D) Stress response regulon with TFBS profiles of MSN2 and FKH2, (E) Carbohydrate metabolism regulon with TFBS profiles of RTG1 and GCN4, and (F) Carbohydrate metabolism genes with TFBS profiles of RTG1 and UME6.

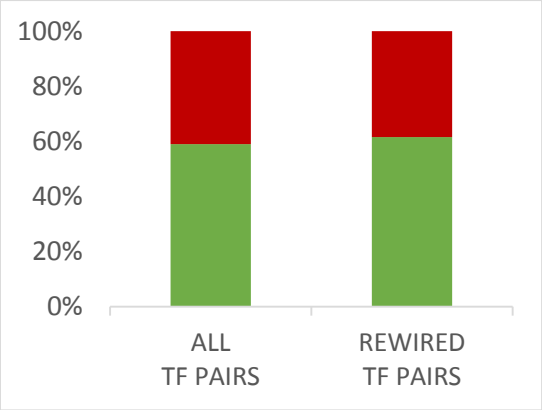


| PHYSICAL INTERACTION POTENTIAL | |
|---|---|
| Odds Ratio | 1.11 |
| Fisher's p-value | 0.14 |

**Figure S7. Physical interaction between rewired TFs in regulons.** Rewired TF-pairs and all other TF pairs are binned into two classes based on propensity for physical interaction based on annotations in STRING database. The plot shows the fraction of TF-pairs that do (green) and do not (red) physically interact. Odds ratio (rewired versus other TF pairs) and Fisher's test p-value (2x2 table) are also shown.

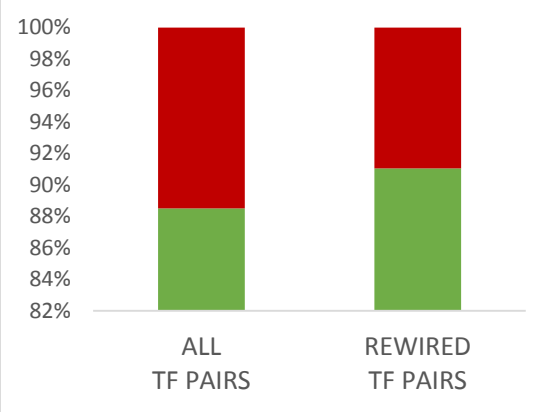


| COMMON UPSTREAM REGULATOR | |
|---|---|
| Odds Ratio | 1.32 |
| Fisher's p-value | 0.002 |

**Figure S8. Proximal shared upstream regulator of rewired TFs in regulons.** Rewired TF-pairs and all other TF pairs are binned into two classes based on their distance to a common upstream regulator. This plot shows the fraction of TF-pairs whose distance to a common UpR is ≤ 4 (green) or > 4 (red). Odds ratio (rewired versus other TF pairs) and Fisher's test p-value (2x2 table) are also shown.

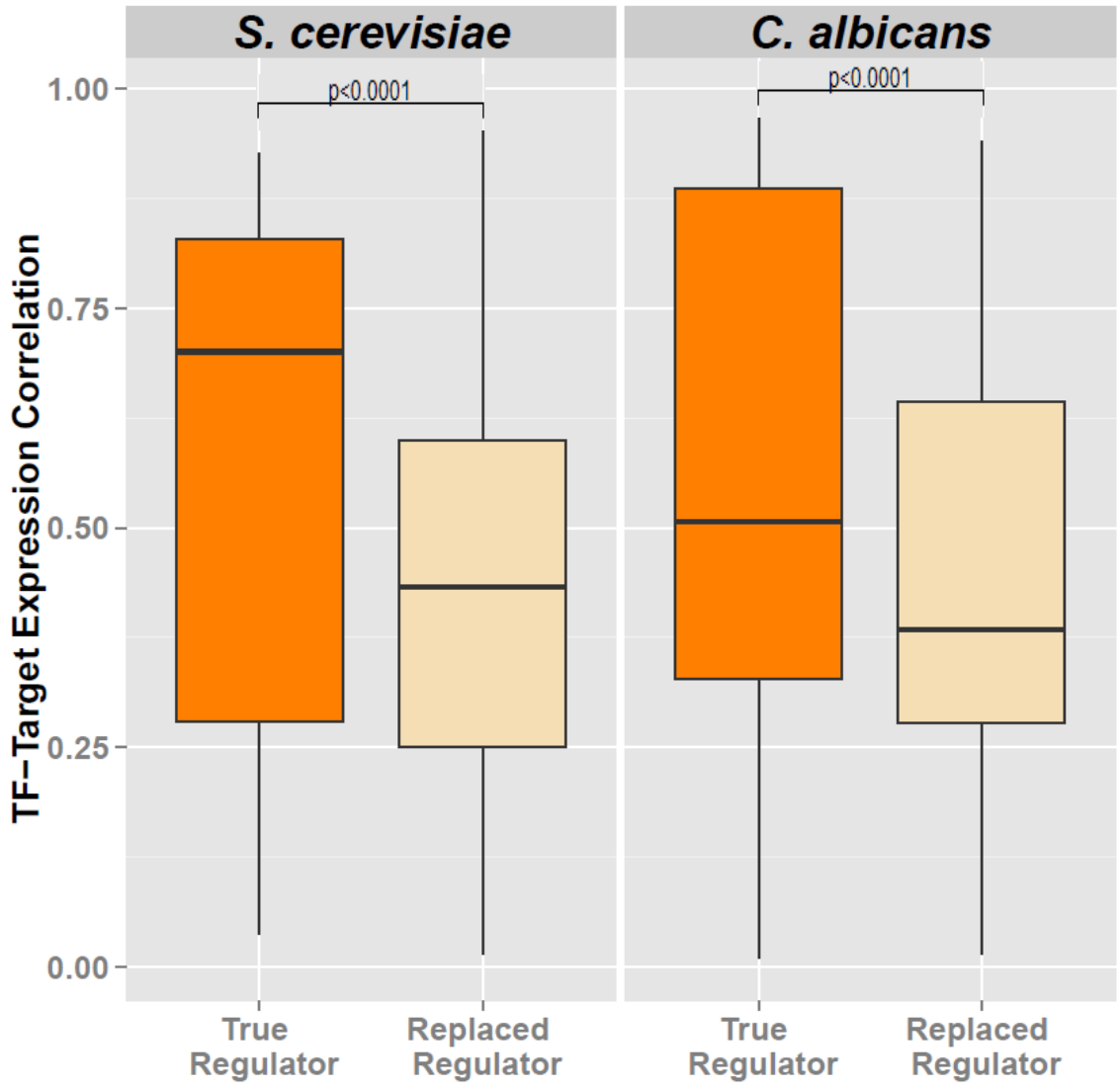


**Figure S9. Species-specific TF-target co-expression for rewiring events detected at branch 11.** The predicted TF-target expression distribution is shown for the TF predicted to be active in a species (dark) and for the TF predicted not to be active (light); the distribution is of all pooled correlations across all significant rewiring events.

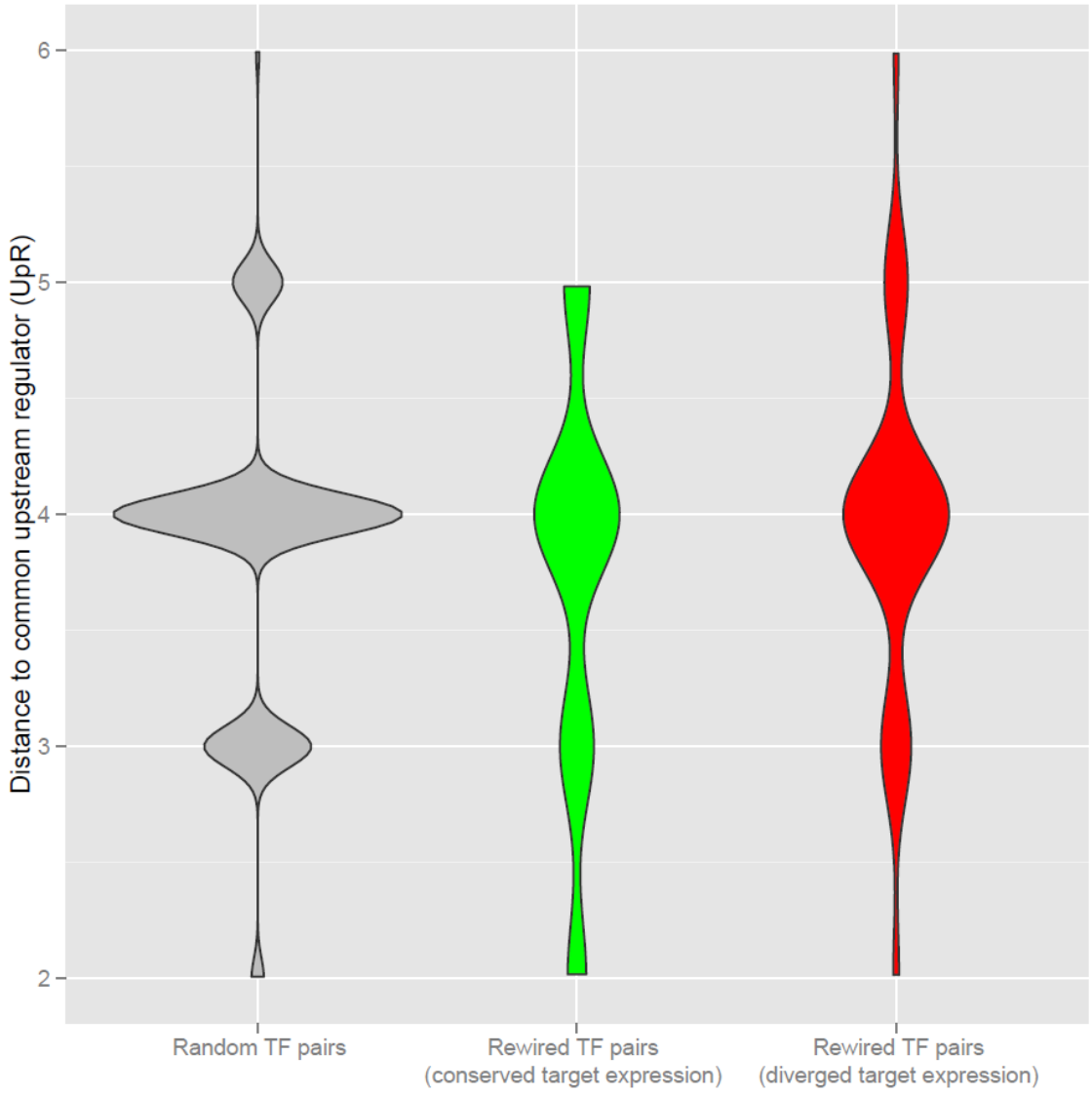


**Figure S10. Distributions of distance (path length) of rewiring TF pairs to their common UpR across species, in different bins of rewiring events segregated based on conservation levels of gene-targets expression.** The target genes of rewiring were binned into conserved (in green) and diverged (in red) expression groups, and their respective distributions of distance to a common upstream regulator is shown in violin plots. As background expectation, the distribution of distance to common UpR for random TF-pairs (in grey) is also shown.

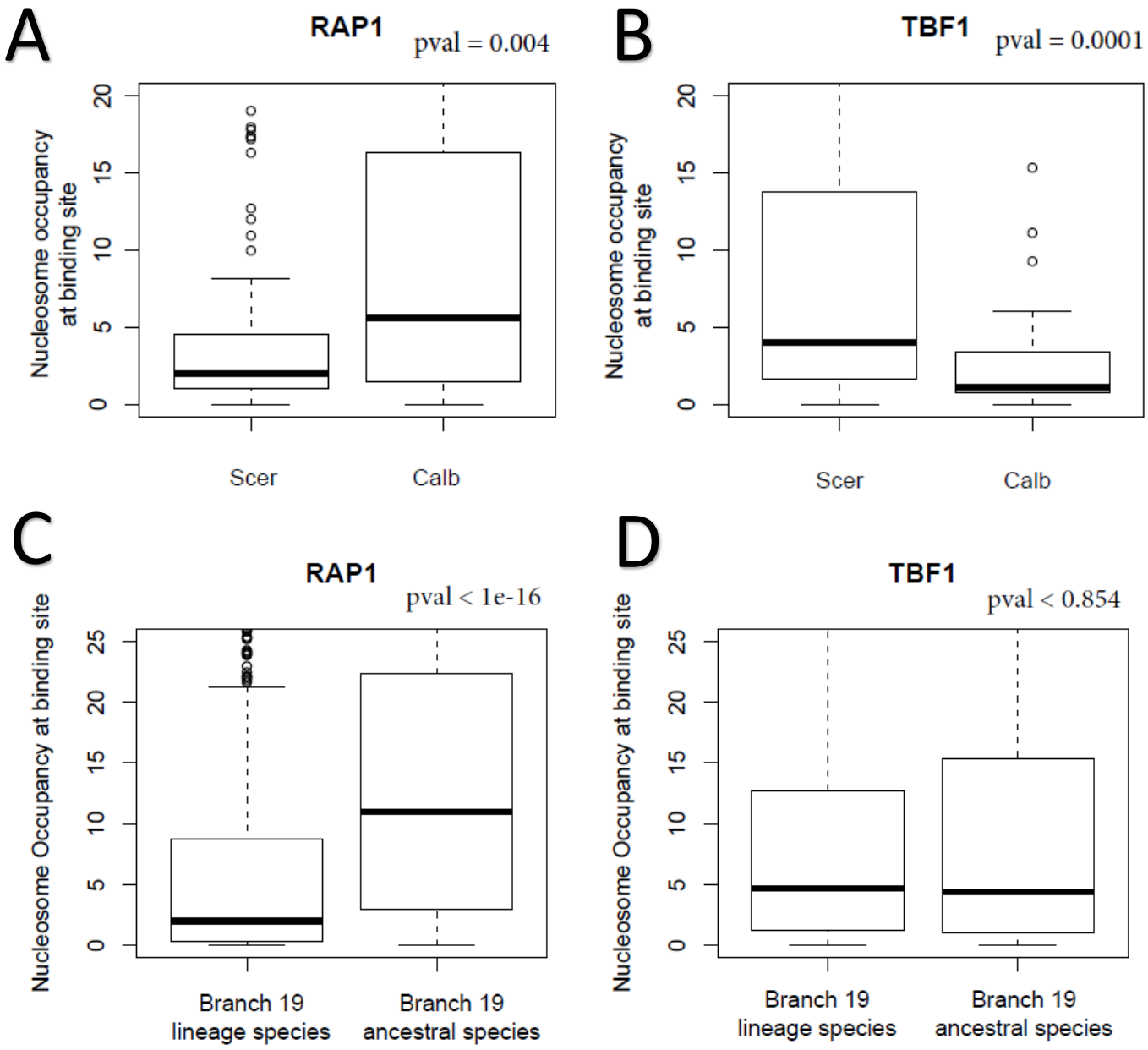


**Figure S11. Nucleosome occupancy of RAP1 and TBF1 at ribosomal genes.** Boxplots showing the distributions of nucleosome occupancy scores (Y axis) at TF binding sites in different yeast species (X axis). **(A)** Nuc. Occupancy at RAP1 sites in *Scer* vs. *Calb*. **(B)** Nuc. Occupancy at TBF1 sites in *Scer* vs. *Calb*. **(C)** Nuc. Occupancy at RAP1 sites in lineage vs. ancestral species. **(D)** Nuc. Occupancy at TBF1 sites in lineage vs. ancestral species. If the known rewiring between *RAP1* and *TBF1* in RP genes is supported by nucleosome occupancy, we expect to see lower nucleosome occupancy for *RAP1* sites in *Scer* and lineage-specific species, compared with that in *Calb* and ancestral species; and vice-versa for TBF1 sites. We find that although these trends are individually consistent in *Scer* and *Calb* (Fig. S8-A, B), we did not observe these patterns in the nucleosome occupancy profiles of *RAP1* vs. *TBF1* binding sites in other species (Fig. S8-C, D) (i.e., there is absence of support across clades despite the fact that this rewiring event spans promoters across all species).

| *Chi-square test (with Yates corr.)* | *#True regulator TFBS - #Replaced regulator TFBS > 0* | *#Replaced regulator TFBS - #True regulator TFBS < 0* | *P-VALUE* |
|---|---|---|---|
| *Implied TFs used* | 65127 | 54858 | $X^2 = 440.73$ |
| *Random TFs used* | 59756 | 60228 | $P < 1 \times 10^{-4}$ |

**Figure S12. Greater motif matches for binding sites of true regulator in rewiring regulons, in a species-specific fashion.** For each rewiring event, we determine the difference between the total number of true regulator binding sites and the total number of replaced regulator binding sites across member genes of a regulon (PWM match score > 80$^{th}$ percentile of all hits), in a species-specific manner. A suitable background expectation is generated by repeating the same using random TF pairs not involved in the corresponding rewiring event. A chi-square test (with Yates correction) shows that binding sites of true regulators are indeed enriched in comparison to those replaced, in a species-specific fashion.

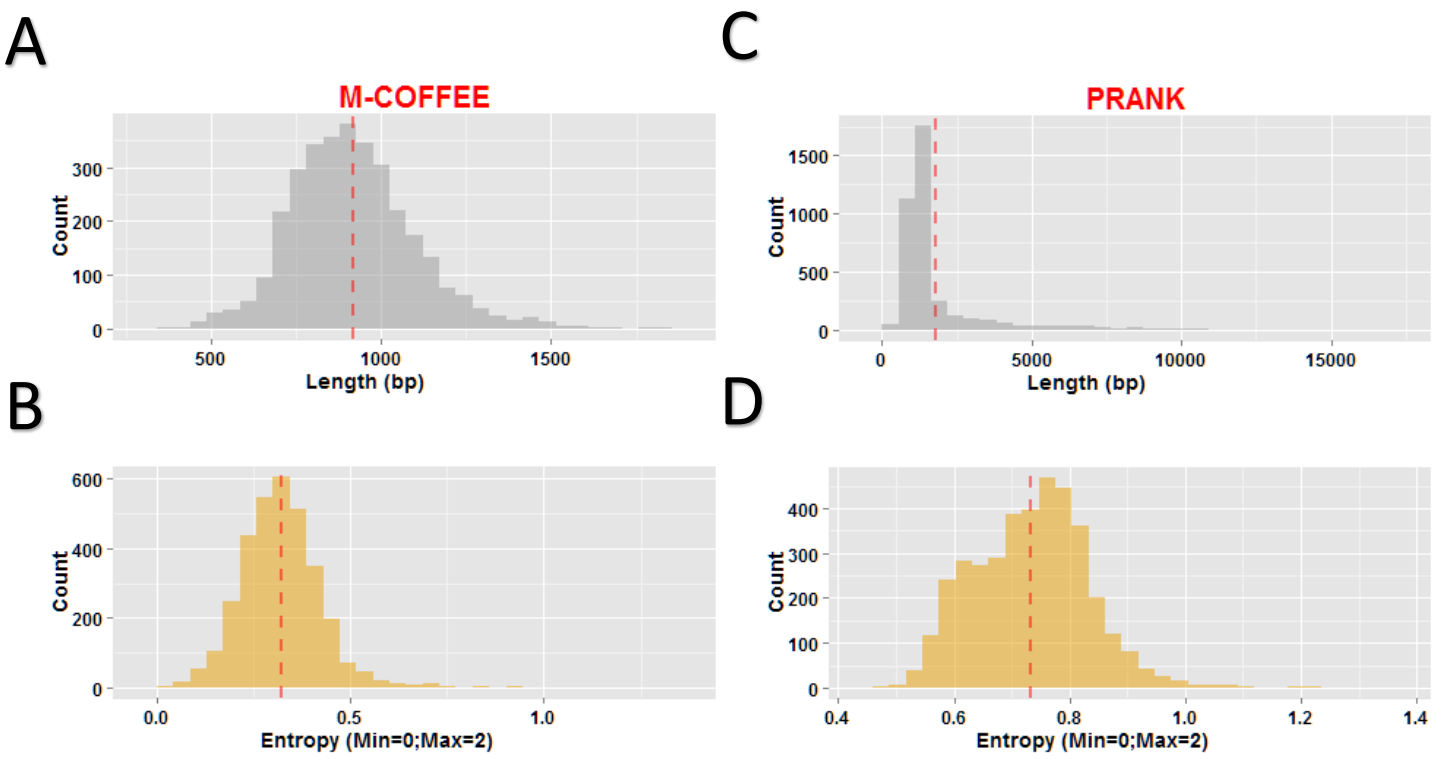


**Figure S13. Length and entropy distribution of reconstructed ancestral sequences.** Two methods were used for generating MSA of extant species, viz., M-COFFEE and PRANK. FASTML was then used in both cases to construct ancestral sequences for each of the 3844 orthogroups at the base of branch 19. **(A)** Length distribution and **(B)** Entropy distribution of ancestral sequences constructed from MSA produced by M-COFFEE. **(C)** Length distribution and **(D)** Entropy distribution of ancestral sequences constructed from MSA produced by PRANK.

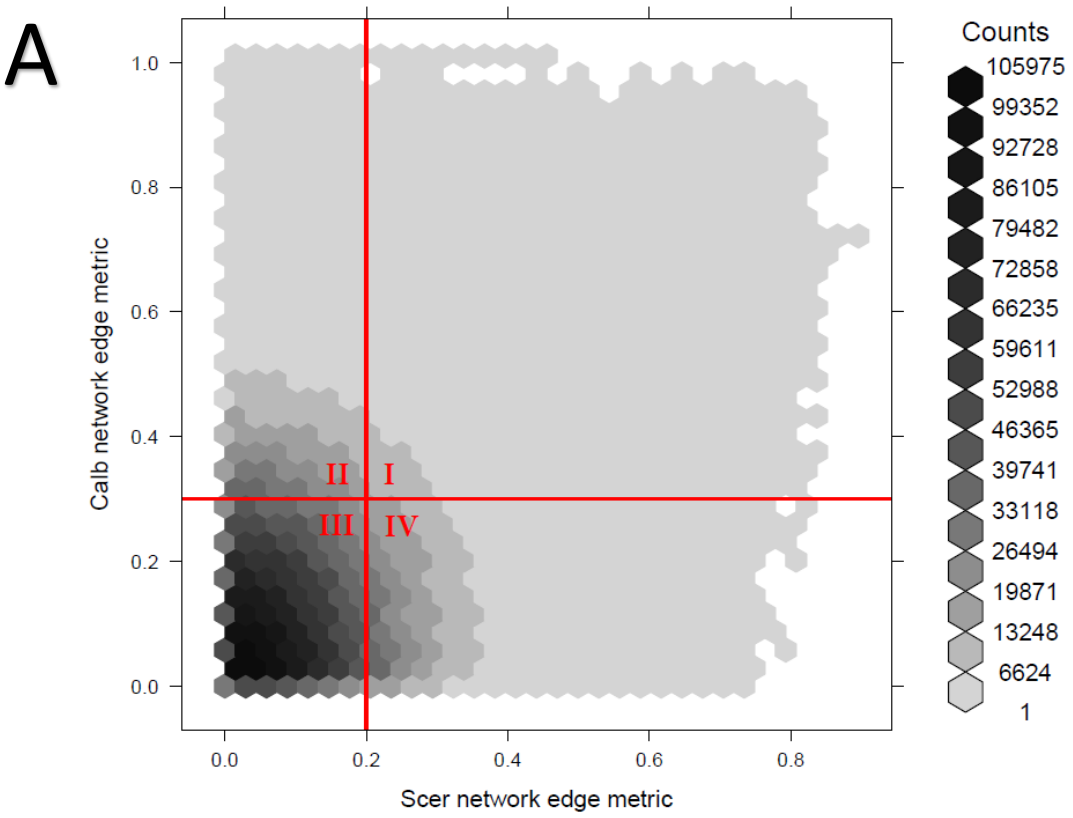


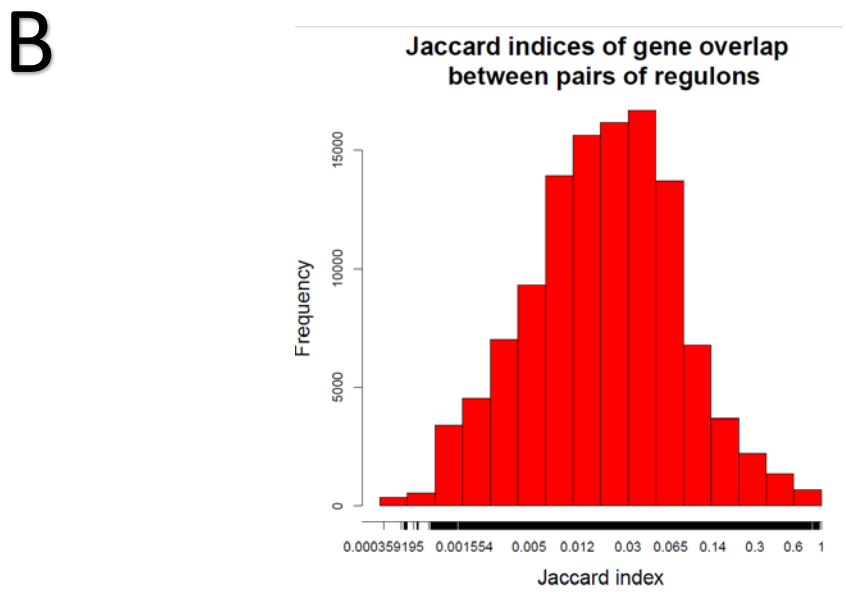


**Figure S14. (A)** A network comprising of a pruned set of edges between genes were used to cluster regulons. Here is shown a density scatter plot of edges (representing expression correlation) between pairs of genes in *Scer* and *Calb* co-expression networks. Each point represents the level of co-expression of a pair of orthologous genes in the *Scer* coexpression network (X axis) and its corresponding level in the *Calb* coexpression network (Y axis) respectively. Datapoints are clustered into hexagons and colored based on point density. All points in quadrant III were discarded from the set of input edges to MCL for regulon clustering **(B)** Histogram of jaccard indices of member genes overlap between pairs of regulons.

| #Significant rewiring events at the gene level for various FDR thresholds | | | | | | |
|---|---|---|---|---|---|---|
| Branch ⇨ FDR ⇩ | **7** | **11** | **19** | **20** | **33** | **39** |
| **0.01** | 1 | 22 | 38 | 186 | 4 | 2 |
| **0.02** | 1 | 38 | 46 | 552 | 4 | 2 |
| **0.05** | 1 | 81 | 120 | 1001 | 4 | 2 |
| **0.1** | 1 | 164 | 228 | 1043 | 8 | 2 |

**Figure S15. Significant rewiring events at the gene level for various FDR thresholds.** The number of rewiring events occurring across internal branch partitions at various FDR thresholds.

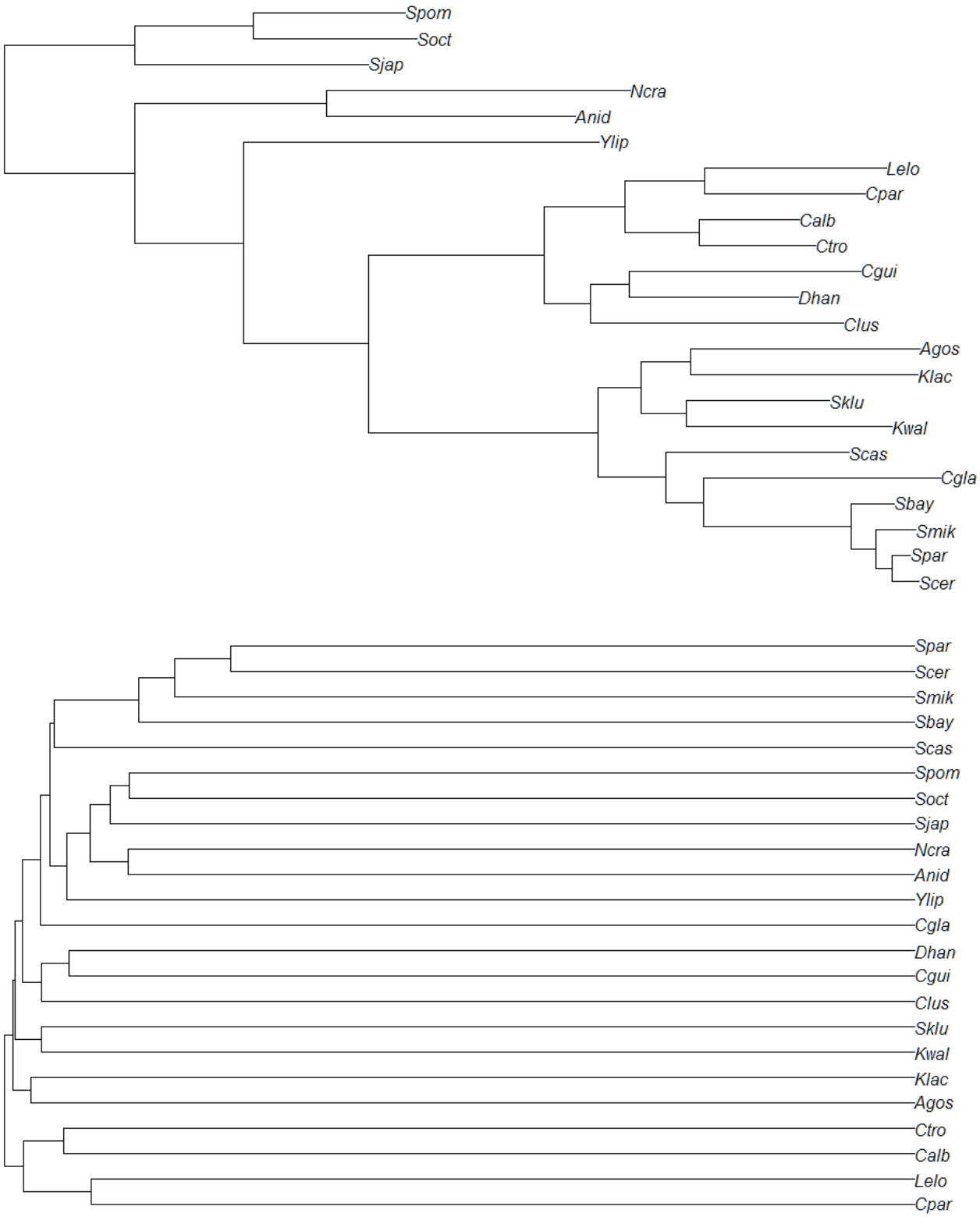


**Figure S16. Yeast species phylogeny trees inferred from aligned genomic blocks and TF binding profiles.** Phylogenetic relationships between 23 yeast species with relative branch lengths. **(A)** Known species phylogeny from genomic sequence, **(B)** Phylogeny derived from clustering binding probability profiles of 176 TFs across orthologous promoters in 23 species.